Assimilation of High-Resolution Satellite-Derived Atmospheric Motion Vectors: Impact on HWRF Forecasts of Tropical Cyclone Track and Intensity

CHRISTOPHER VELDEN AND WILLIAM E. LEWIS

Cooperative Institute for Meteorological Satellite Studies, University of Wisconsin–Madison, Madison, Wisconsin

WAYNE BRESKY

I.M. Systems Group, Rockville, Maryland

DAVID STETTNER

Cooperative Institute for Meteorological Satellite Studies, University of Wisconsin–Madison, Madison, Wisconsin

JAIME DANIELS

NOAA/NESDIS Center for Satellite Applications and Research, College Park, Maryland

STEVEN WANZONG

Cooperative Institute for Meteorological Satellite Studies, University of Wisconsin–Madison, Madison, Wisconsin

(Manuscript received 16 June 2016, in final form 7 November 2016)

ABSTRACT

It is well known that global numerical model analyses and forecasts benefit from the routine assimilation of atmospheric motion vectors (AMVs) derived from meteorological satellites. Recent studies have also shown that the assimilation of enhanced (spatial and temporal) AMVs can benefit research-mode regional model forecasts of tropical cyclone track and intensity. In this study, the impact of direct assimilation of enhanced (higher resolution) AMV datasets in the NCEP operational Hurricane Weather Research and Forecasting Model (HWRF) system is investigated. Forecasts of Atlantic tropical cyclone track and intensity are examined for impact by inclusion of enhanced AMVs via direct data assimilation. Experiments are conducted for AMVs derived using two methodologies (''HERITAGE'' and ''GOES-R''), and also for varying levels of quality control in order to assess and inform the optimization of the AMV assimilation process. Results are presented for three selected Atlantic tropical cyclone events and compared to Control forecasts without the enhanced AMVs as well as the corresponding operational HWRF forecasts. The findings indicate that the direct assimilation of high-resolution AMVs has an overall modest positive impact on HWRF forecasts, but the impact magnitudes are dependent on the 1) availability of rapid scan imagery used to produce the AMVs, 2) AMV derivation approach, 3) level of quality control employed in the assimilation, and 4) vortex initialization procedure (including the degree to which unbalanced states are allowed to enter the model analyses).

1. Introduction

Given the increasing volume and resolution of satellite data now becoming available, it is desirable to seek optimal methods to exploit these observations. This is especially pertinent to improving forecasts of high-impact weather events such as tropical cyclones (TCs). One type of geostationary satellite data that can be expected to improve the representation of TC wind structure and its environmental flow fields is atmospheric motion vectors (AMVs). AMVs are derived from sequential satellite images by tracking coherent cloud and water vapor targets (Velden et al. 1997), and are an approximation of the local wind at the target height. They are assimilated routinely in all operational global numerical weather prediction systems and have been shown to produce positive impacts on the accuracy of global model initial conditions (e.g., Le Marshall et al. 2008a) and forecasts of tropical cyclone track (Velden

Corresponding author e-mail: Christopher Velden, chrisv@ssec.wisc.edu

DOI: 10.1175/MWR-D-16-0229.1

et al. 1998; Goerss 2009; Langland et al. 2009; Berger et al. 2011).

Methods to process and improve the quantity and accuracy of AMVs are evolving (Velden et al. 2005; Bresky et al. 2012; Borde et al. 2014). Higher-spatiotemporal-resolution data are being realized through advancing satellite sensors and scanning strategies, increased computing resources for processing the data, and improving derivation methodologies. More frequent dataset availability and improved AMV quality is now possible with rapid image scanning strategies becoming routine on operational geostationary satellites. Near ''full disk'' (scanning view of the satellite) AMV datasets are becoming increasingly available on an hourly basis from operational/national global processing centers. Even more frequent AMV datasets (1–10 min) are now possible over programmable targeted areas when a ''rapid scan'' mode is activated on the satellite. While these higher-spatiotemporal-resolution datasets are likely not suited for coarser-resolution global model assimilation systems, regional/mesoscale models can benefit. For example, Le Marshall et al. (2008b) documented the impacts of high-resolution AMVs in the operational Australian regional model, and the Japan Meteorological Agency (JMA) found that the assimilation of MTSAT rapid scan AMVs in their mesoscale model with four-dimensional variational data assimilation (4D-Var) provided improvements to typhoon forecasts (Yamashita 2012). Using research-quality regional modeling systems, Pu et al. (2008) found positive impact of assimilating AMVs on TC forecasts, and Wu et al. (2014, 2015) used the Weather Research and Forecasting (WRF) Model and Data Assimilation Research Testbed (DART) assimilation system to more closely examine AMV forecast impacts on TC tracks and intensity. They developed data processing and assimilation strategies that achieved optimal results, and some of these are employed in this study.

Data assimilation (DA) specific to TCs has advanced rapidly in recent years, focusing on the assimilation of a variety of data including airborne Doppler radar and inner-core dropwindsondes, surface best track data (TCVitals), and upper-ocean observations. Given the promise of advanced imagers on geostationary satellites that are now becoming reality [e.g., *Himawari-8/9*, *GEO-KOMPSAT-2A/2B*, EUMETSAT-MTG, GOES-R (launched 19 November 2016 and is now *GOES-16*)], it is prudent to take advantage of improving data assimilation schemes to seek optimal methods of fully exploiting the information content of these data in high-impact weather events such as TCs. In particular, the impact on analyses/forecasts of TC intensity and track from assimilation of high-resolution AMVs into the operational WRF system for hurricane prediction [Hurricane Weather Research and Forecasting Model (HWRF); Tallapragada et al. (2014)] is the focus of this study.

A basic description of the AMV datasets, model/DA, and selected TC cases is given in section 2. Section 3 is an overview of the methodology employed and the experiments conducted. Model forecast impact results are presented in section 4, followed by a summary and discussion of the findings in section 5.

2. Background

At the beginning of this study, operationally produced AMVs by NOAA/NESDIS were being directly assimilated into only one of the operational HWRF's three domains (i.e., d02, the coarsest of the vortex-following nests). Most of the information content of these AMVs must first pass through the sieve of the National Centers for Environmental Prediction (NCEP) Global Data Assimilation System (GDAS), where they can then impact the HWRF background fields. However, the GDAS assimilates AMVs using data thinning and quality-control (QC) strategies commensurate with the purposes of global analyses and likely does not retain full AMV information on smaller flow scales associated with TCs (Sears and Velden 2012). Consequently, our research is aimed at providing guidance to NCEP/EMC and other regional DA and modeling centers on how to most effectively extract the wind information from AMVs in the context of TC environments.

a. AMV datasets

AMVs are routinely processed by NOAA/NESDIS from the two operational geostationary (GOES-East and -West) satellites. These datasets are generated to provide large-scale coverage, with the primary beneficiary being global model assimilation with nominal 6-h cycles. For global completeness, similar AMV datasets are produced by EUMETSAT from the European Meteosat series, and by JMA over the western Pacific region from the MTSAT/Himawari satellites. Countries such as India, Korea, and China now also have geostationary satellite systems that provide regular AMV datasets. All of these sources are routinely made available over the Global Telecommunication System (GTS).

While the operationally produced AMV datasets are reliable and adequate for global model analyses, the coverage and processing methodologies are not optimized for smaller-scale flows. Regional model/DA systems such as those designed for numerical hurricane

forecasting are trending toward nested grids down to cloud-resolving scales. High-impact local weather events such as TCs may have important mesoscale flow fields that need to be resolved in order to improve these high-resolution analyses and subsequent forecasts. Therefore, it is imperative to develop observation strategies that meet these increasing demands.

One emerging way to enhance the coverage, density, and quality of AMVs is by taking advantage of new-generation satellite sensors and scanning capabilities. More rapid scanning, coupled with higher-precision sensors and image navigation allow for improved feature tracking with higher density and higher quality AMVs. Traditionally, the operational AMV datasets noted above employ image triplets separated by 30 min. More recent satellites such as the current GOES series, *Himawari-8*, Meteosat-SG, and *COMS-1* allow routine imaging at 10–15 min, and super-rapid scanning down to 1-min intervals over targeted regions. Since clouds and water vapor features evolve in time, it is desirable to sample them at the shortest interval possible to obtain the most coherent AMVs (Velden et al. 2005). GOES-R, which was launched on 19 November 2016, will be commissioned for use in 2017 and is referred to as *GOES-16*. It will be possible to routinely sample TC events at up to 1-min frequency in multispectral imagery for storms within the *GOES-16* field of view.

As part of GOES-R risk reduction and readiness, an effort is under way to develop improved AMV processing methodologies that are designed to optimize the information content of the observations in TC environments. The HWRF Model analyses and forecasts provide the test bed to evaluate different processing and assimilation strategies. While the chosen experiments were not conducted in real time, all attempts were made to simulate the operational environment to the extent possible.

The enhanced AMV datasets used in this study were generated for selected hurricane cases with fully automated procedures using two different processing routines: a traditional approach that is based on the current NOAA/NESDIS operational processing strategies (''HERITAGE''), and a new approach being implemented for AMV processing in the GOES-R series era (''GOES-R''). These AMV datasets contain estimates of wind speed and azimuth as derived from infrared window (IR), shortwave infrared (SWIR), visible (VIS), and water vapor at high cloud top (CTWV) imagery (no clear-sky WV vectors were produced for this study). The VIS (daylight hours) and SWIR (nighttime hours) AMVs are only processed to track lower-tropospheric (700–1000 hPa) clouds. GOES rapid scan images are employed in the AMV tracking process when available. The HERITAGE method includes an elaborate automated QC procedure tuned to hurricane environments, which is invoked in postprocessing (Velden et al. 1998). The GOES-R approach employs a novel nested tracking technique with improved vector height assignments, and relies on a quality indicator that is based on a set of QC tests. Further details on the HERITAGE approach can be found in Velden et al. (2005), and a description of the GOES-R approach in Bresky et al. (2012). Both AMV processing methodologies are evaluated in this study for their dataset attributes in TC environments, and ultimately their impact on HWRF analyses and forecasts.

1) PROCESSING DETAILS SPECIFIC TO HURRICANE ENVIRONMENTS

For each of the three selected TC cases in this study (further described in section 2c), enhanced AMV datasets were reprocessed using both of the aforementioned methods for the full life cycle of the storm (with the exception of Sandy) at hourly intervals, and over a domain centered on the TC. Example plots for each selected TC are shown in Fig. 1 with respect to the HWRF d02 assimilation domain (the actual datasets extend beyond the plotted boundaries, except for Sandy, which was restricted by the *GOES-14* super rapid scan domain).

The AMV processing strategies for enhanced observations around TCs were patterned after the study by Velden et al. (1998) and include the use of GOES rapid scan imagery to derive the vectors whenever available (further discussed in the results section). Briefly, the strategies include the following: 1) adjusting the target selection and search box criteria to allow denser AMV coverage to better capture smaller-scale TC flow fields; and 2) with the HERITAGE method, a relaxation of the QC postprocessing step in the vicinity of a targeted TC. The HERITAGE processing method is regulated by an objective analysis with operating parameters that have been tuned and QC settings that have been relaxed to increase the retention of vectors in those regions of the TC and its environment that may deviate from the background guess fields but still be in spatial coherence with neighboring observations [see Velden et al. (1998) for further processing details, and Sears and Velden (2012) for dataset characteristics].

It should be noted that the GOES-R series AMV processing algorithm is relatively new, and as such does not yet benefit from years of empirical tuning for hurricane applications. The quality control step consists of a single parameter, the quality indicator (QI; Holmlund et al. 2001), and the ramifications of this will become evident in the results section. The adaptation of this methodology is still a work in progress, but the improved vector

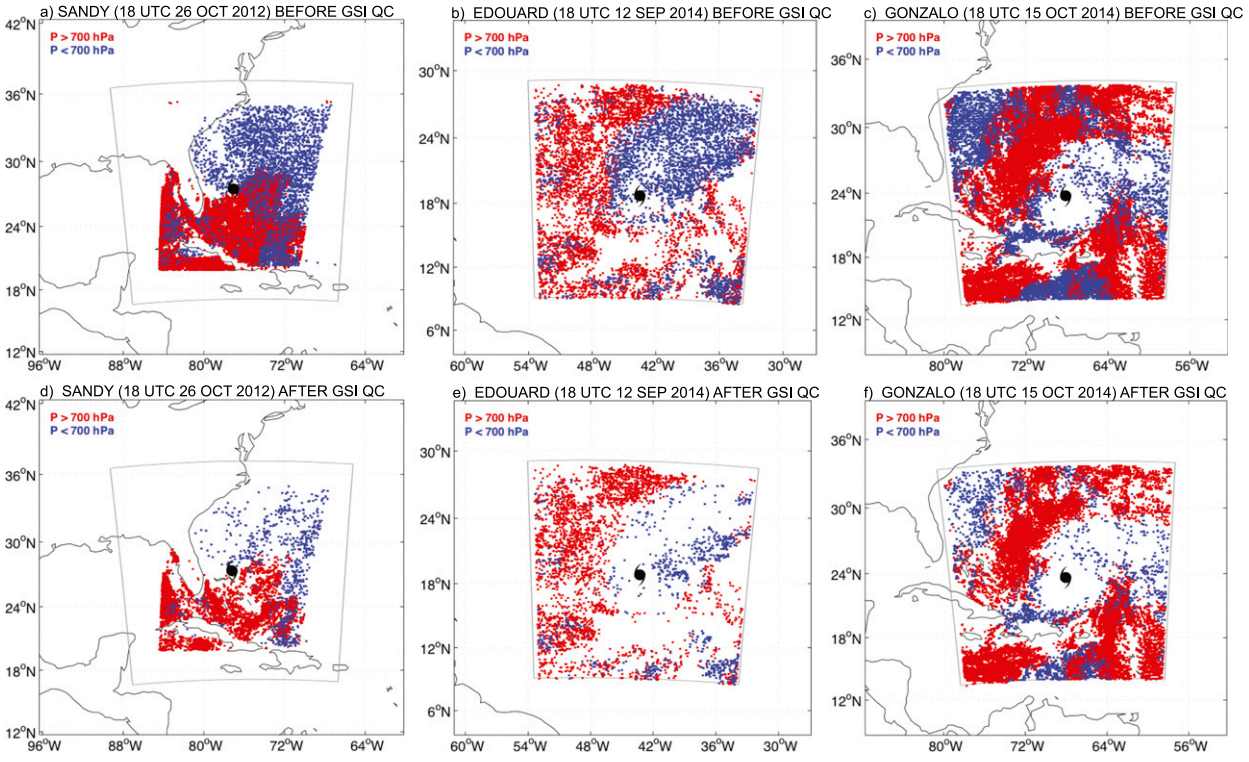

FIG. 1. Example plots of enhanced AMVs assimilated into HWRF (d02 domain indicated) for the three TC cases in this study. (a)–(c) Before and (d)–(f) after GSI QC is applied. The AMVs plotted are derived from the GOES-R method.

derivation and height assignments warranted a comparison with the existing operational (HERITAGE) method.

2) DATASET PREPARATION FOR ASSIMILATION

Once the datasets were processed, the native file formats were converted to ASCII text and then encoded into the GDAS prepbufr files for inclusion in the HWRF DA. AMVs over land and between 400 and 700 hPa were excluded based on the study by Sears and Velden (2012), which showed higher vector errors in this height range. Since the typical vertical distribution of AMVs in the tropics is highly bimodal (cirrus level and marine cumulus level), the volume of data excluded was quite small. Finally, only vectors that surpassed empirically determined thresholds of QI were passed on to the prepbufr files per the studies of Wu et al. (2014, 2015).

b. Model description, initialization, and data assimilation

1) THE HWRF MODEL

All simulations were conducted using HWRF version 3.6 obtained from the trunk in HWRF developers' repository on 1 November 2014. With the exception of customary bug fixes and the computing platform employed (see below), this essentially represents the FY2014 operational HWRF code (hereafter H214).

The H214 configuration comprises three computational grids: a parent domain (hereafter d01) with 0.18° spacing, and two TC-following, nested domains at 0.06° (hereafter d02) and 0.02° (hereafter d03) spacing, respectively. The horizontal extent of the domains is 80° × 80°, 12° × 12°, and 7.1° × 7.1° respectively. Each of the domains has 61 vertical levels, and the model top is set at 2 hPa.

Cloud microphysics is simulated using a version of the Ferrier scheme (Ferrier 2005) optimized for hurricane applications, and the GFS aimplified Arakawa–Schubert (SAS) (e.g., Han and Pan 2011) scheme is used to parameterize deep and shallow convection on d01 and d02. Convection is handled explicitly on d03. Additional physics packages used in this study include the following: the GFDL land surface model (Tuleya 1994) and radiation schemes (Fels and Schwarzkopf 1975; Lacis and Hansen 1974; Schwarzkopf and Fels 1991); the GFS boundary layer scheme (Hong and Pan 1996); and ocean coupling is accomplished via the Message Passing Interface Princeton Ocean Model for Tropical Cyclones (MPIPOM-TC; Yablonsky et al. 2015).

A more complete description and summary of the FY2014 operational version of the HWRF model

physics and numerics may be found in the H214 scientific documentation (Tallapragada et al. 2014).

2) MODEL INITIALIZATION

Preparation of HWRF for a TC forecast involves a mixture of static field interpolation, vortex relocation/enhancement, and data assimilation/merging. The first two items will be covered in this section, and the latter will be detailed in the next section.

On the parent domain, d01, large-scale fields from the GFS analysis are interpolated to the model grid both horizontally and vertically prior to *every* forecast (i.e., no further optimization or data assimilation is performed). On the moving nests, d02 and d03, the first-guess fields come from the GDAS 6-h forecast. To this first guess is added a bogus vortex (if it is the first forecast cycle for this particular TC), or a relocated, cycled vortex (if a prior 6-h HWRF forecast for this TC exists). In addition to relocation, enhancement of the vortex structure (maximum wind, wind radii) may take place if the cycled and observed vortex characteristics are appreciably different. In each case, the basis for the observed TC vortex parameters (position, intensity, wind radii) is established by the NCEP TC-Vitals message valid at a particular date and time.

3) DATA ASSIMILATION

In addition to the model initialization steps mentioned above, 6-hourly cycling DA is performed on the expanded HWRF d02 and d03 domains to produce a vortex structure, which more closely fits the observations (the expanded domain d02 and d03 domains are $20° \times 20°$ and $10° \times 10°$, respectively, allowing observations which lie outside the $10° \times 10°$ and $7.1° \times 7.1°$ forecast domains to impact the analysis). After analyses are obtained on the expanded domains, the results are merged to the forecast domains using the standard "blending initialization" as included in the H214 code package. It is important to note that the blending process has a significant impact on the vortex structure used to initiate forecasts. In particular, analysis increments within 150 km of the center are eliminated below 600 hPa in favor the first-guess structure provided by vortex initialization. The full benefits of data assimilation are only fully realized beyond the blending zone (i.e., >300 km from the vortex center).

DA in H214 makes use of the hybrid variational technique option in the Gridpoint Statistical Interpolation analysis system (GSI) (Wu et al. 2002; Wang 2010). Background error covariances are derived from a combination of ensemble-based and static sources. The HWRF DA system (HDAS) uses an 80-member GFS ensemble to generate the ensemble-based covariance, and the static component relies on the same static covariances used for NCEP's GFS model. The hybrid approach permits a degree of flow dependence in the covariance structure (and, likewise, in the analysis increments) that is not possible with a strictly static approach. The background error covariance used in HDAS is a weighted sum of the ensemble and static components such that the former accounts for 80% and the latter accounts for 20% of the final value.

For this study, the GSI code was used for all experiments. To establish an upper bound with respect to impact, no GSI-specific thinning was done on the AMV observations prior to assimilation (thinning of various degrees could be introduced later if necessary and used as a tuning parameter in future work). The default horizontal/vertical thinning was retained for all other observations.

Prior to the execution of each outer loop, the GSI employs a standard QC gross error check that eliminates observations outside of set tolerances from the background field (the previous 6-h forecast plus the vortex relocation/adjustment). The GSI QC scheme is a function of observation error, and in our study the AMV errors were decreased as suggested in Nebuda et al. 2014. This results in a more restrictive gross-error check, and the effect of this is shown in Fig. 1 by a reduced vector density (GOES-R AMV examples are plotted). To test the bounds of AMV impact on HWRF analyses/forecasts, the default tolerances of the GSI QC scheme were relaxed for one set of experiments (described further in section 3). In these "NO-QC" experiments, almost all AMV observations that pass internal processing QC (also discussed in section 3) are permitted to pass through the HDAS gross error checks. Further information on the HDAS may be found in the H214 scientific documentation (Tallapragada et al. 2014).

c. *Selected case study TCs*

Three Atlantic TCs were selected for study based on a number of factors that include the availability of satellite rapid scan imagery and the degree of forecast difficulty with respect to both track and intensity. The three storms selected are Hurricanes Sandy (2012), Gonzalo (2014), and Edouard (2014). Figure 2 shows the tracks of these storms along with their intensity trends (from NHC best track records).

Hurricane Sandy was notorious for its sharp, highly anomalous westward turn and making landfall along the U.S. mid-Atlantic seaboard. The storm was also characterized by convective structure transformations leading to intensity fluctuations during its life cycle, making this a challenging system to forecast (Blake et al. 2013). Fortuitously, the *GOES-14* satellite was tasked for

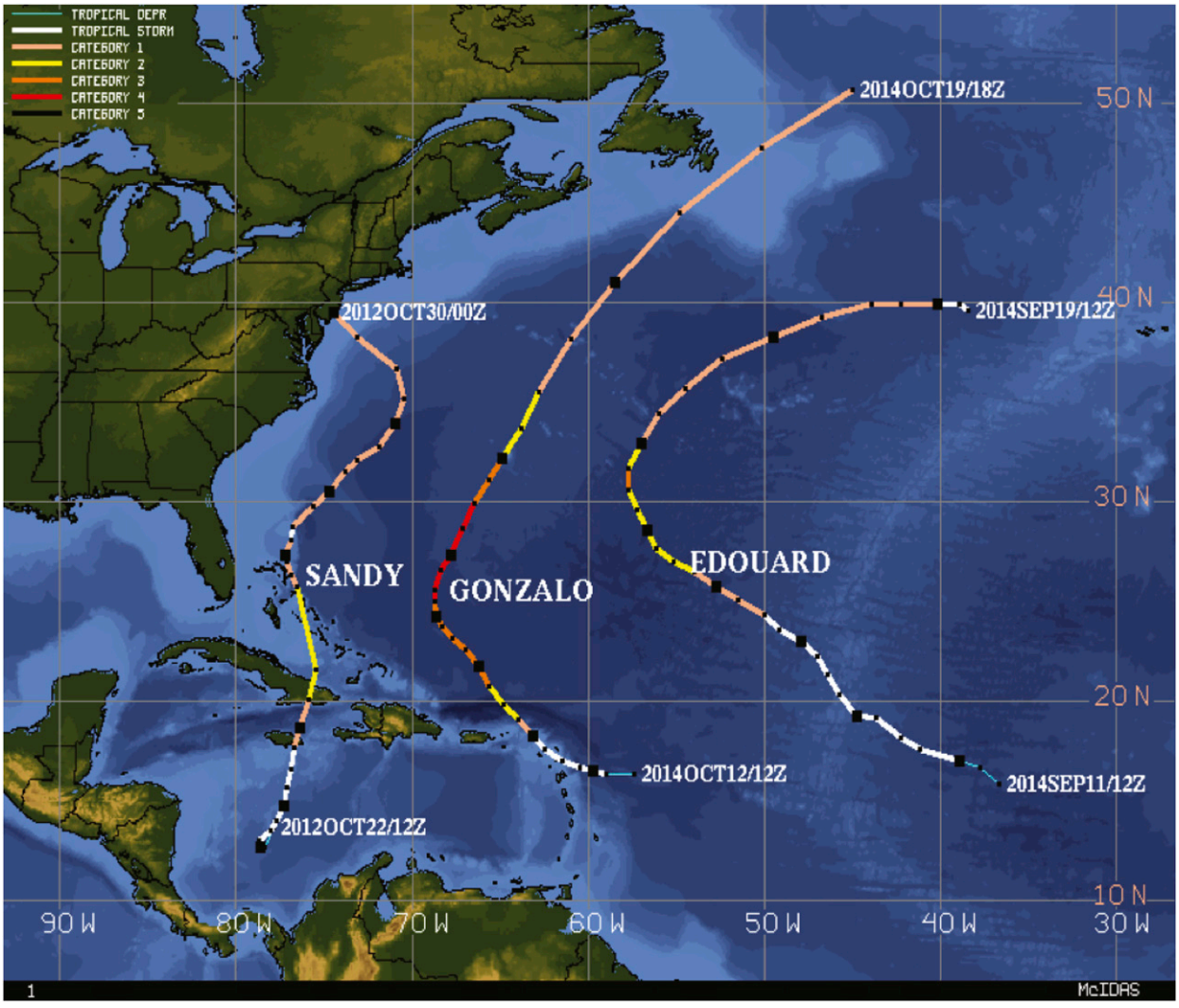

FIG. 2. Tracks and intensities for the three TC cases in this study (from NHC best tracks).

Super Rapid Scanning Operations (SRSO) by NOAA/NESDIS for the period from Sandy's passage over Cuba until after its U.S. landfall. Continuous 1-min images centered on Sandy were provided by *GOES-14*, offering an unprecedented 5-day period of such observations during a historic TC. This case also serves as an excellent demonstration of image sampling that will become routine now that *GOES-16* is operational.

Gonzalo formed east of the Lesser Antilles and quickly strengthened into a category 4 hurricane (on the Saffir–Simpson hurricane wind scale), and made landfall in Bermuda as a high-end category 2 hurricane, causing extensive damage. The NHC forecast and much of the model guidance did not predict Gonzalo to strengthen as quickly as it did during the first few days of its existence (Brown 2015). Limited Rapid Scan Operations (RSO, 7-min image frequency) were active for *GOES-13* during most of Gonzalo's lifetime. However, the RSO domain only covers west of ~60°W. East of 60°W, only 15-min imagery was available for AMV derivations.

Edouard was a category 3 hurricane at peak intensity that remained over the open Atlantic Ocean during its lifetime. This storm was relatively well behaved, so both official and most model guidance was better than average for both track and intensity (Stewart 2014). In addition, there was no satellite rapid scanning available at any time, so that the derivation of AMV datasets relied on the routine 15-min imagery available from *GOES-13* and *Meteosat-10*.

3. Methodology

The enhanced AMV datasets for this study were created by CIMSS and NOAA/NESDIS/STAR, and

encoded into the GDAS prepbufr files for inclusion in the cycling DA workflow. [It should be noted that the nominal spatial density of the enhanced AMV datasets processed in this study is on the order of 10–20 km (spectral and cloud target dependent), which is 2–3 times denser than typical global operationally processed AMV datasets.] These AMV datasets contain observations of speed and azimuth as derived from IR, SWIR, CTWV, and VIS channel imagery and were converted to zonal and meridional wind components prior to their insertion into the prepbufr files. In addition, as part of dataset preparation, the AMV datasets were first passed through a prefilter step before entering the data assimilation system following the procedure of Wu et al. (2014). This step is in accord with the following criteria: the enhanced AMVs are passed on to the assimilation only if the associated QIs are equal to or larger than an empirically determined 0.6. AMVs meeting this QI threshold but with expected error (EE) values $>4.5\,\mathrm{m\,s^{-1}}$ are filtered out unless the AMV is $>25\,\mathrm{m.s^{-1}}$ and has an attending QI > 0.7. The QI and EE values are produced during the AMV derivation process and represent internal QC indicators of AMV quality.

As noted earlier, the reprocessed AMV datasets are derived at a frequency of 1 h, but the HWRF data assimilation cycle is 6-hourly. Rather than assume that all observations falling within the data assimilation window (± 3 h) are valid at the analysis time, HWRF uses first-guess at appropriate time (FGAT) to produce background fields that are valid at each observation time. Doing so produces innovations (observations minus background), which more faithfully represent the information content of the observations themselves and allows the computation of increments that reflect the injection of that information into the analysis. To accomplish this, FGAT uses HWRF forecasts valid 3 h prior and 3 h subsequent to the analysis time, which, when combined with the forecast valid at the analysis time itself, produces a set of three forecast fields that can be used to interpolate the HWRF background to any arbitrary time within 3 h of the analysis. Using this procedure, the ''off cycle'' AMV datasets can be assimilated more effectively.

As discussed above, two methods of AMV derivation are investigated for impact (HERITAGE and GOES-R). Both algorithms are employed to produce AMV datasets during the life cycle of the three chosen TC cases described above to illuminate some of the possibilities of the GOES-R series mission relative to the problem of TC prediction. Baseline performance is first established by generating a Control (CTL) set of HWRF forecasts. This involves cycling data assimilation (as described above) from the first date/time of each TC with an available TCVitals message, and continuing until the TC has either dissipated or become extratropical. In order that the impact of the AMV observations might be most effectively isolated (see the results section below), only radiosonde observations (RAOBs) from the GDAS prepbufr file are assimilated on the moving nests (i.e., d02 and d03) during this first set of CTL simulations. Observation errors for the RAOBs are as given in the HDAS error table.

To assess the potential impact of the AMVs in a more realistic operational setting, a second set of Control forecasts are produced. This baseline (CTL ALL) assimilates the full set of conventional observations used in the operational HWRF as of 2014, except for the operationally produced AMVs. In the results section below, we also include the operational HWRF forecasts (labeled as H214), which were the real-time runs for TCs Gonzalo and Edouard, and a postprocessed set of runs for TC Sandy done by NCEP/EMC using the same H214 code. Table 1 summarizes the characteristics of the HWRF Control/baseline experiments presented in this study.

The subsequent model impact experiments then add the HERITAGE or GOES-R AMV observations, respectively. As noted earlier, observation errors for the AMVs were modified from the values given in the HDAS error table based on results from previous research (Nebuda et al. 2014), which indicated that a reduction in the errors used in the standard GSI error table yielded a tighter fit of the analysis to the data. The vertical structure of the observation errors used in this study is shown in Fig. 3 and represents a 30% reduction relative to the default error table values.

As mentioned above, a final modification to the normal HDAS workflow was made in the GSI quality control of the AMV datasets. While no alteration was made for the CTL or the CTL ALL experiments, in the AMV impact experiments two separate QC settings were explored. The first used the same GSI default settings employed in CTL, while the second (NO-QC) altered (relaxed) the gross error check in the following manner. Observations are rejected if the following inequality is satisfied:

$$|\mathbf{y} - H\mathbf{x}| > e_{\mathrm{gross}} \times \{\max[e_{\mathrm{min}}, \min(e_{\mathrm{max}}, e_{\mathrm{obs}})]\},$$

where $|\mathbf{y} - H\mathbf{x}|$ is the magnitude of the innovation (or ''observation minus background''), e_{gross} is the gross error parameter, e_{min} is the minimum error parameter (fixed at 1.4), e_{max} is the maximum error parameter (fixed at 20.0), and e_{obs} is the observation error (as depicted in Fig. 3). In this study, NO-QC used $e_{\mathrm{gross}} = 10.0$ (whereas the default setting is $e_{\mathrm{gross}} = 1.3$). Using these

TABLE 1. Baseline HWRF simulation attributes. CTL is Control/baseline, and H214 is the operational HWRF as of 2014. Here d02 and d03 refer to the two HWRF TC-following nested domains.

	Conventional (excluding raob) on d02 and d03	Raob on d02 and d03	Satellite (excluding operational AMV) on d02 only	Operational AMV on d02 only
H214	✓	✓	✓	✓
CTL		✓		
CTL ALL	✓	✓	✓	

values, the maximum allowable innovation magnitudes range from ~15 m s^{-1} in the lower troposphere to near 50 m s^{-1} in the uppermost troposphere. This means that the NO-QC experiment essentially permits all but the most egregious outliers (and allows a fuller examination of the AMV impact). It is worth noting that GSI is a 3D-Var system with explicit assumptions of linearity and Gaussianity. Some of the outlying observations in NO-QC (particularly those generating innovations greater than, say, 3σ from the background) may be difficult for GSI to fit properly on this account and the results should be interpreted with this in mind.

Table 2 summarizes the characteristics and attributes of the HWRF AMV impact experiments presented in this study.

4. Results

The results of the HWRF forecasts of TC track and intensity (defined as maximum sustained surface winds, or Vmax) are first presented for the concatenated sample of the three TC case study events versus a Control set of forecasts with reduced conventional observations assimilated (CTL). This set of experiments is designed to show the impact the AMVs can have on the HWRF analyses and forecasts in the absence of competing data sources. The second set of assimilation experiments are benchmarked against the full set of operational data (CTL ALL) and the operational HWRF (H214) in order to provide a more realistic assessment of the AMV observation impacts. For this set of experiments, the results are also broken down by TC cases to diagnose situational differences. It should be noted that very few of the data impact results are statistically significant at the 95% level, primarily due to the relatively small forecast sample sizes.

a. AMV forecast impacts versus CTL

Figure 4a shows the results of the aggregated forecasts from the three TC events for overall track errors. The results versus CTL show some modest positive impact from the AMV assimilation with the GOES-R method out to about 66 h, after which time results are mixed. Regarding the aggregated intensity forecast errors, Figs. 4b–d indicate that both AMV processing methods yield near-neutral results during the first 24-h forecast lead times, then modest positive impacts between 36 and 96 h, then mixed results after that out to 120 h. It is apparent from these three cases that the assimilation of the enhanced AMVs (particularly the new GOES-R datasets) show some promise to reduce HWRF forecast errors (owing to small sample sizes, none are statistically significant at the 95% level), but it appears difficult to produce impact at the short forecast range (first ~24 h) and toward the end of the 5-day forecast range (further speculation on potential reasons for this is discussed in the summary section).

Also shown in Fig. 4 are the results of the experiments with the GSI QC tolerances greatly relaxed (NO-QC). It is readily apparent that the more stringent and tuned internal QC associated with the HERITAGE AMV processing method limits the differences between the respective HERITAGE experiment results. On the other hand, assimilation of the GOES-R datasets, which rely only on the QI parameter for internal QC, greatly benefits from the application of the GSI QC step.

b. AMV forecast impacts versus "all-obs" CTL

The results presented above were benchmarked against a CTL with only radiosonde observations assimilated in order that the potential impact of the AMV

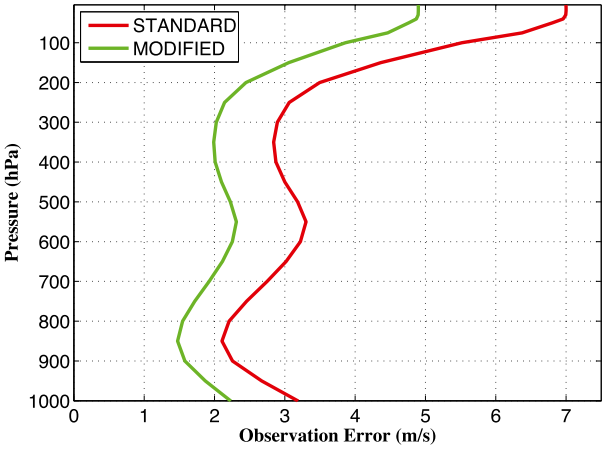

FIG. 3. The vertical structure of AMV observation errors used in this study (green). The default GDAS values are shown in red for comparison.

TABLE 2. HWRF AMV impact simulation attributes. HERITAGE represents the legacy GOES AMV processing method, while GOES-R is a contemporary AMV processing approach developed as part of the GOES-R series algorithm working group; d02 and d03 refer to the two HWRF TC-following nested domains.

	Parent baseline	Enhanced AMVs—HERITAGE method on d02 and d03	Enhanced AMVs—GOES-R method on d02 and d03	GSI QC (i.e., gross error check)
HERITAGE NO-QC	CTL	✓		
HERITAGE	CTL	✓		✓
GOES-R NO-QC	CTL		✓	
GOES-R	CTL		✓	✓
HERITAGE ALL	CTL ALL	✓		✓
GOES-R ALL	CTL ALL		✓	✓

observations might be most effectively isolated. To assess the impact of the AMVs in a more realistic operational setting, a second set of Control forecasts (CTL ALL) was produced, which assimilated the identical set of observations used in the operational H214, except for the operationally produced AMVs. The operational AMVs were left out of the CTL ALL since they were not routinely assimilated at the time of the three TC events, and to avoid redundancy issues in subsequent experiments when the enhanced AMV datasets processed by CIMSS are added. Based on the findings in section 4a, only the results of the

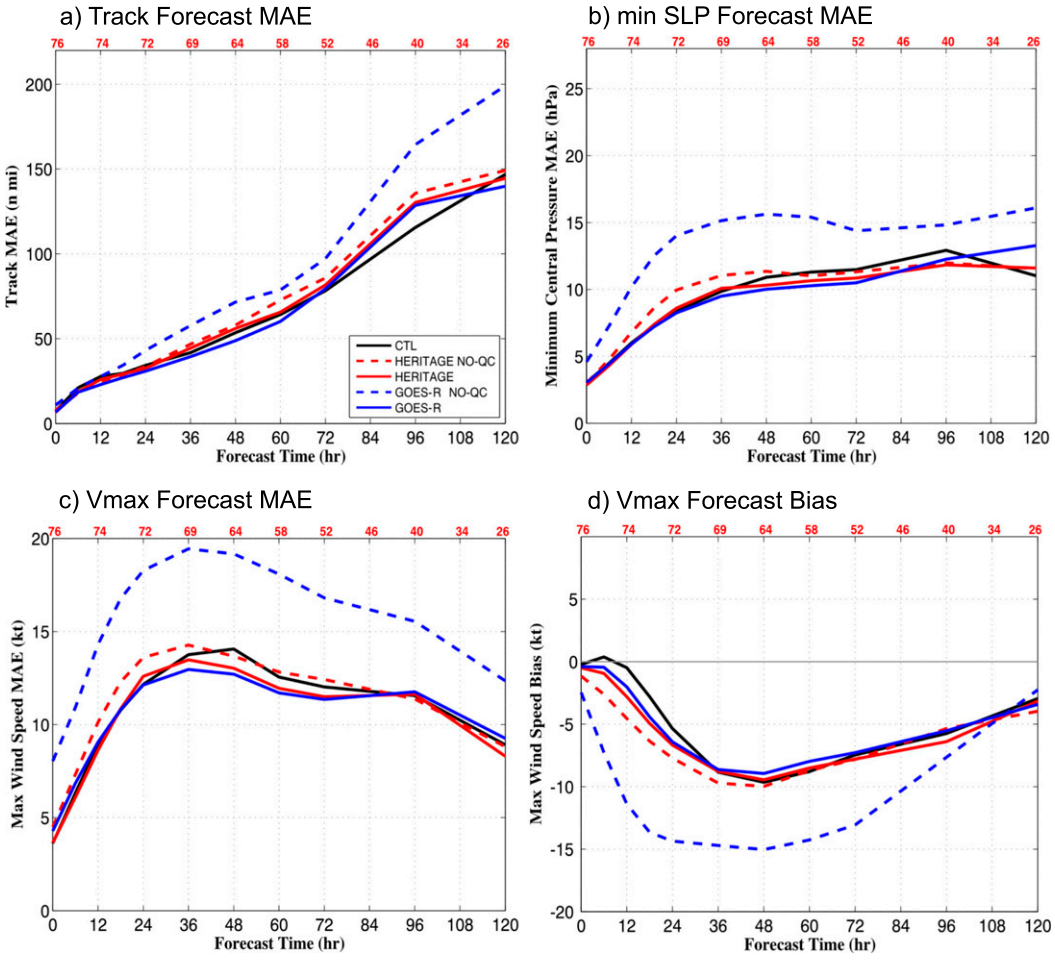

FIG. 4. Mean absolute error (MAE) of (a) HWRF forecast track, (b) forecast minimum SLP, (c) forecast maximum sustained wind, and (d) forecast maximum sustained wind bias for CTL and the CTL series impact experiments. Sample sizes for each forecast lead time are indicated in red along the top of the plot.

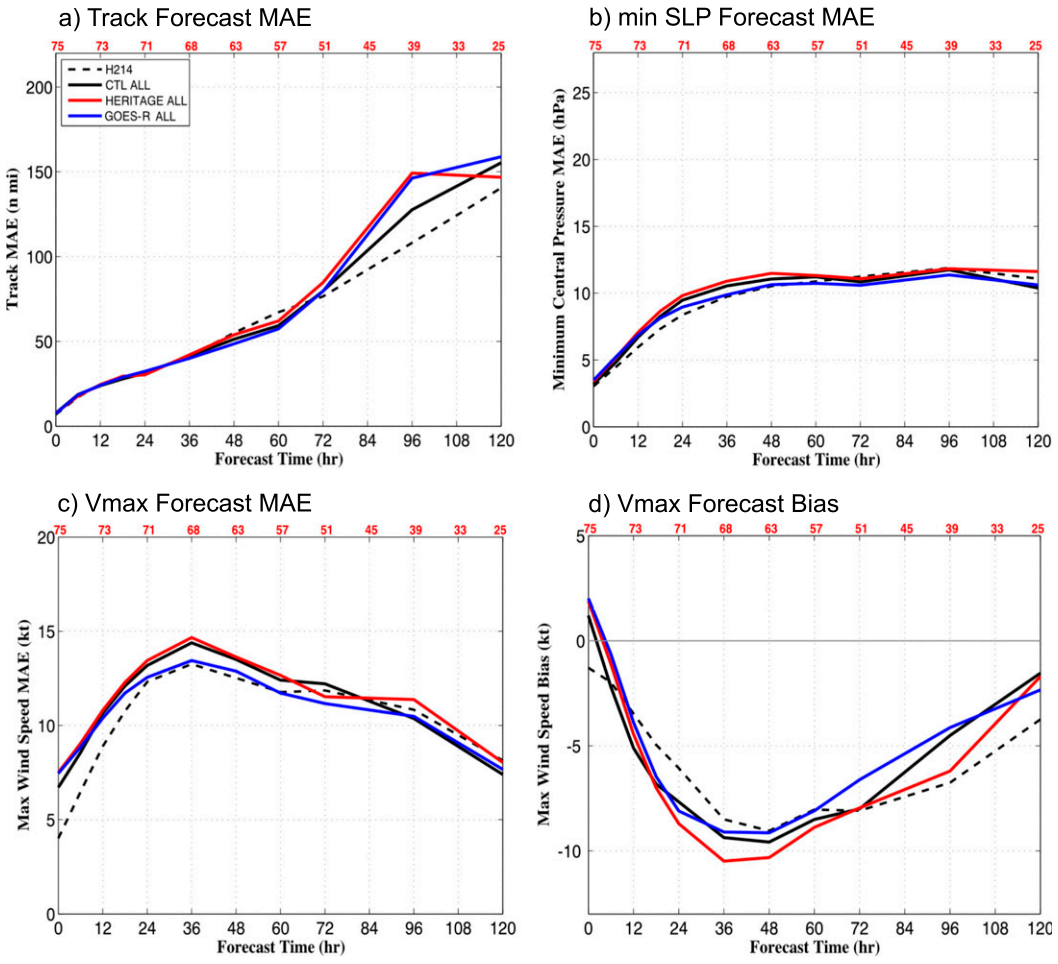

FIG. 5. As in Fig. 4, but for CTL ALL and the CTL ALL series impact experiments. H214 is included for comparison purposes only and does not serve as the baseline for any impact experiment(s).

experiments with the GSI default QC fully invoked are presented in this section.

Not surprisingly, Fig. 5a shows that the modest positive AMV impacts on HWRF track forecasts out to about 72 h are reduced when compared to the "full-obs" CTL ALL. The notable degradation at 96 h is curious, and will need to be verified with a much larger sample size for significance. A more promising result is shown in Figs. 5b–d for HWRF intensity forecasts. Even against the more stringent CTL ALL, there is a notable reduction in forecast errors in the 24–96-h lead time range with the assimilation of GOES-R AMV datasets. Before and after this range, the impacts are negligible, as was the case versus the basic CTL.

Another way to view the HWRF forecast results is by examining the pairwise frequency of superior performance, or FSP. This metric provides the percentage of times that one experiment is superior to the other in terms of forecast error. For example, Figs. 6a and 6b show how often the HWRF AMV experiment forecasts are superior to CTL ALL for track and intensity. Above 50% indicates a positive impact. For the track forecasts, the HERITAGE experiments are slightly negative overall, while the GOES-R results are mixed. The impact on intensity shows a little more promise in both methods, with the GOES-R achieving slightly better results. This can also be seen in Figs. 6c and 6d, where the two AMV experiments (full GSI QC) are paired against each other. The GOES-R experiment is a solid winner in the both the intensity and forecast track comparison.

It is informative to further dissect the general findings of the aggregate results presented above by examining the forecast impacts from the individual storm events, given the diversity in the case selection.

1) HURRICANE SANDY (2012)

The track and intensity forecasts for Hurricane Sandy after its passage over Cuba and eventual westward turn

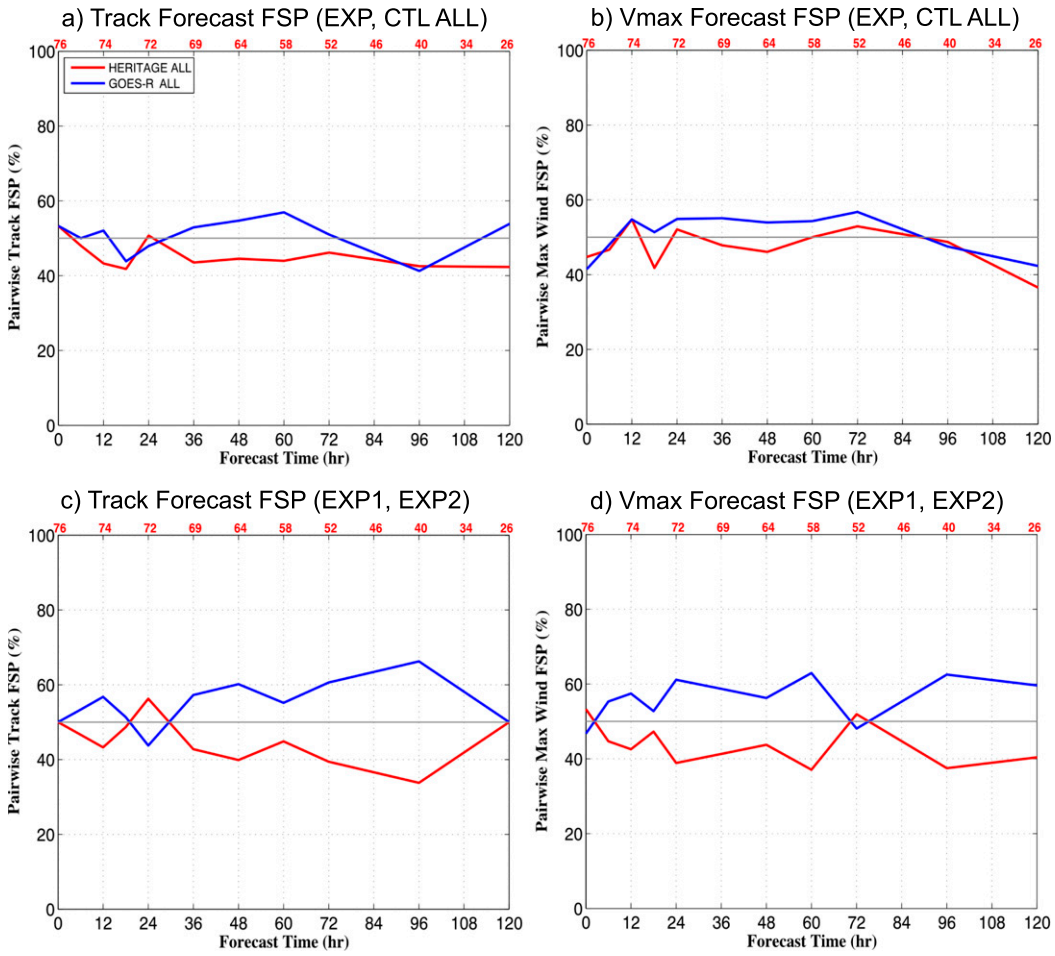

FIG. 6. Frequency of superior performance (FSP) for the pairwise (i.e., two member) comparison of CTL ALL and individual impact experiments for (a) forecast track and (b) forecast maximum sustained wind speed, and for the pairwise comparison of HERITAGE ALL and GOES-R ALL for (c) forecast track and (d) maximum sustained wind speed. EXP = HERITAGE ALL (EXP1) is in red, and GOES-R ALL (EXP2) is in blue. Sample sizes for each forecast lead time are indicated in red along the top of the plot.

into the U.S. eastern seaboard were complex and well documented (Blake et al. 2013). Sandy's TC structure changes and highly uncertain track due to rapidly evolving environmental steering flows (high track bifurcation potential; McNally et al. 2014) made this a natural case to examine for potential AMV impacts. In addition, the *GOES-14* satellite was activated for 1-min continuous image sampling (SRSO) during this segment of Sandy, allowing for optimal target tracking in processing of the AMV datasets. It should be noted, however, that the optimal image intervals for most effective tracking was found to be 3 min for VIS and 5 min for IR/SWIR/CTWV.

Figure 7a shows the 120-h forecast results of directly assimilating the enhanced AMVs into HWRF for Sandy's track versus CTL ALL. The results of the HWRF reruns of this case by NCEP using the operational H214 model code (which assimilates a large array of conventional and satellite observations) are also shown for comparative purposes. It is noteworthy that these benchmark track forecasts errors are considered quite low [below average for 2012 Atlantic TCs, Blake et al. (2013); NHC forecast verification statistics]. Despite this, there is a minor positive impact from both the HERITAGE and GOES-R methods when compared with CTL ALL (and H214) out to around 72 h. Beyond 72 h, the AMV results slightly degrade versus the CTL ALL forecasts, although the sample size becomes very small. In this case, the comparison of track forecast results between the two AMV processing methodologies (HERITAGE and GOES-R) is mixed.

The HWRF intensity forecasts for Sandy are shown in Figs. 7b–d. Overall the results are mixed, with the AMVs improving the forecasts at some lead times and

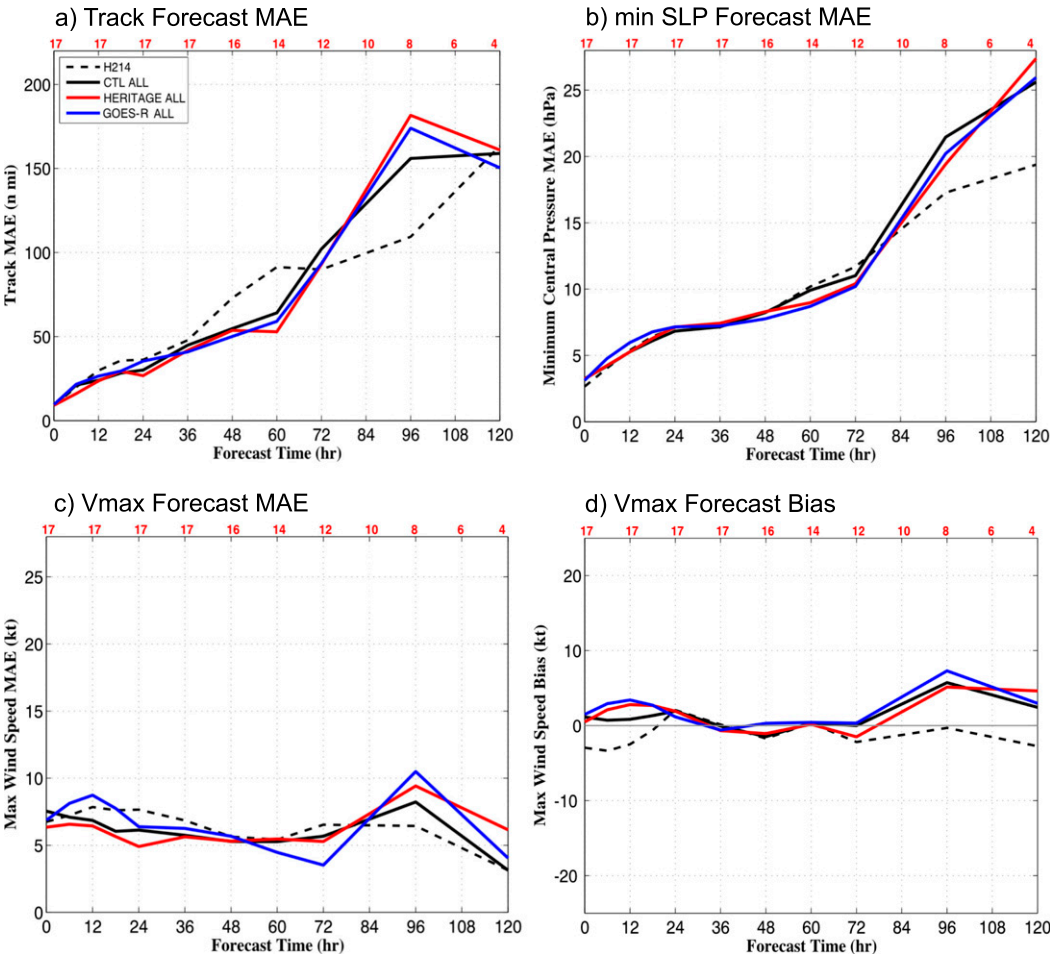

FIG. 7. As in Fig. 5, but for the Hurricane Sandy case only.

degrading at others. Except for around 72 h, the HERITAGE method performs slightly better than the GOES-R approach with respect to the maximum surface wind speed (Vmax) mean forecast errors. This may be a result of the HERITAGE processing method being better adapted to rapid scans based on extensive research and development.

2) HURRICANE EDOUARD (2014)

Since Edouard occurred primarily over the central Atlantic and out of reach of most conventional observations, it is a good case to highlight the potential of enhanced AMVs to impact HWRF forecasts. Figure 8a shows there is a small but consistently positive impact on track forecast errors with the GOES-R AMV assimilation versus CTL ALL for the 24–120-h period, and for all but the 84–108-h period versus the operational HWRF (H214). Impacts are neutral for the HERITAGE experiment.

With regards to Edouard's intensity forecasts, Figs. 8b–d show generally neutral impacts from the GOES-R experiment while HERITAGE slightly degrades the intensity forecasts. A large percentage of the HWRF mean Vmax errors for Edouard are due to a negative bias (Fig. 8d), and the assimilation of the HERITAGE AMVs actually aggravates this bias.

It should be noted that no rapid scan imagery was available during Edouard. The AMVs relied on images at regular 15-min intervals from GOES and Meteosat. Since vector quality improves with reduced image intervals (Velden et al. 2005), we can speculate that the results in this case likely represent a lower bound on model forecast impact potential as we enter the GOES-R series era when rapid-scanning will be the "new normal."

3) HURRICANE GONZALO (2014)

The HWRF benchmark track forecasts for Gonzalo were phenomenal, with a mean error of only 37 n mi (1 n mi = 1.852 km) at 48-h lead time [5-yr-average NHC track error (2009–13) is 78 n mi]. Therefore, it is not surprising that the assimilation of AMVs were not

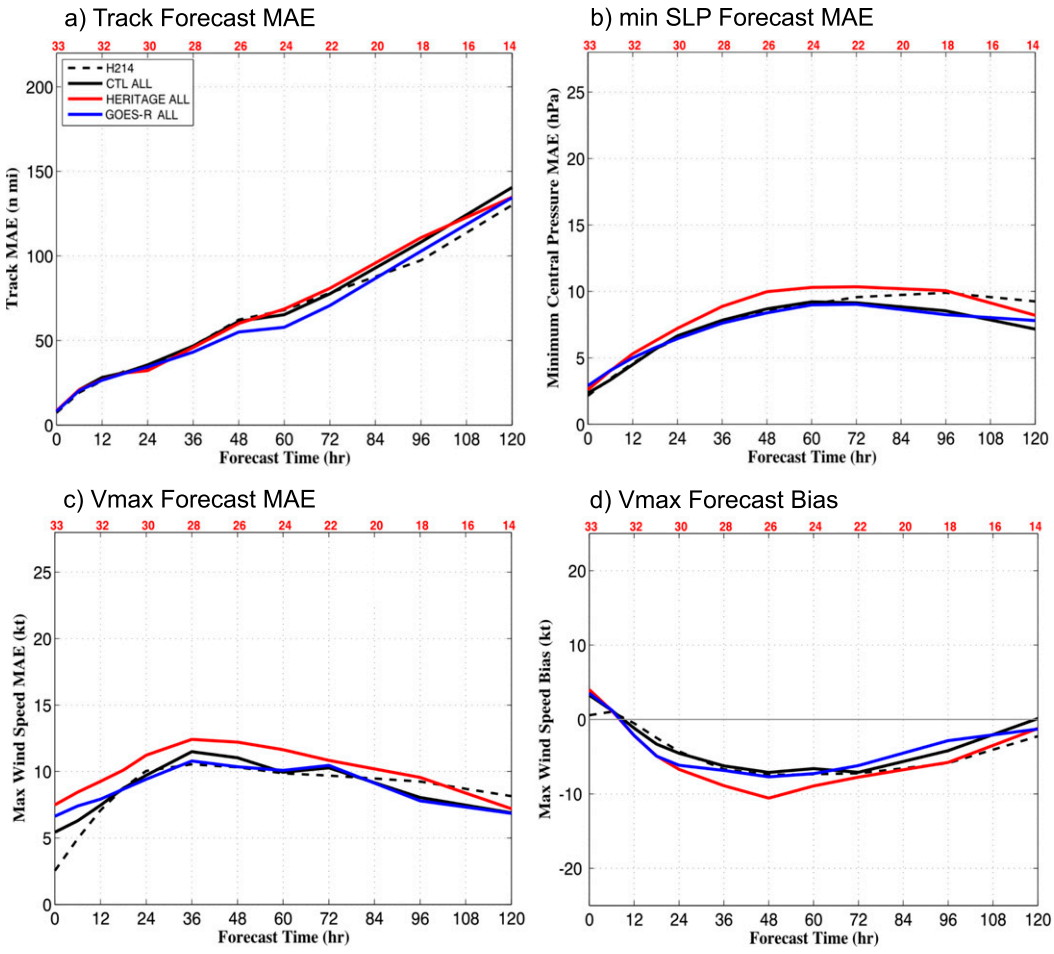

FIG. 8. As in Fig. 5, but for the Hurricane Edouard case only.

positively impactful; in fact some forecast degradation is noted at the longer lead times (Fig. 9a). The GOES-R algorithm dataset performance is slightly superior to the HERITAGE method out to 72 h.

The HWRF intensity forecasts for Gonzalo are another matter. Figures 9b–d shows the mean Vmax forecast errors rapidly jump up to 20–25 kt during the first 36-h lead times in both the CTL ALL and operational (H214) runs. As with Edouard, most of this error is due to a strong negative bias (Fig. 9d). The assimilation of AMVs, especially the GOES-R datasets, notably reduces the errors relative to the CTL ALL. There were rapid scans available for most of the event duration (regular GOES RSO, which provides nominal 7.5-min image updates). This factor could be contributing to the positive intensity forecast impacts.

c. *Diagnosing impact causes*

It is beyond the scope of this paper to conduct an exhaustive analysis of the model behavior with respect to the forecast results presented above. Indeed, such a diagnosis is complicated at the very outset by the extensive vortex processing that occurs in HWRF both prior to (i.e., relocation and size/intensity correction) and after (i.e., merging/blending) data assimilation. The former tends to obliterate flow dependence and impedes the recursive accumulation of observation impact in the background, while the latter discards observation impact present in the analysis. Despite these difficulties, a single instance is presented to shed some light on how the AMVs are impacting the results in a particular case. Figure 10 shows an example from Hurricane Sandy for the analysis valid at 0000 UTC 26 October 2012. Relative to CTL, the GOES-R AMV experiment (cf. Figs. 10e and 10b) produces deeper, more robustly anticyclonic wind increments (i.e., positive north of the center, negative south of the center) on expanded domain d02. This serves to weaken the TC's cyclonic circulation and corrects the positive (i.e., too strong) intensity bias evident in the CTL at this time. The succeeding 6-h HWRF background field (valid at 0600 UTC 26 October 2012) suggests that the correction is a

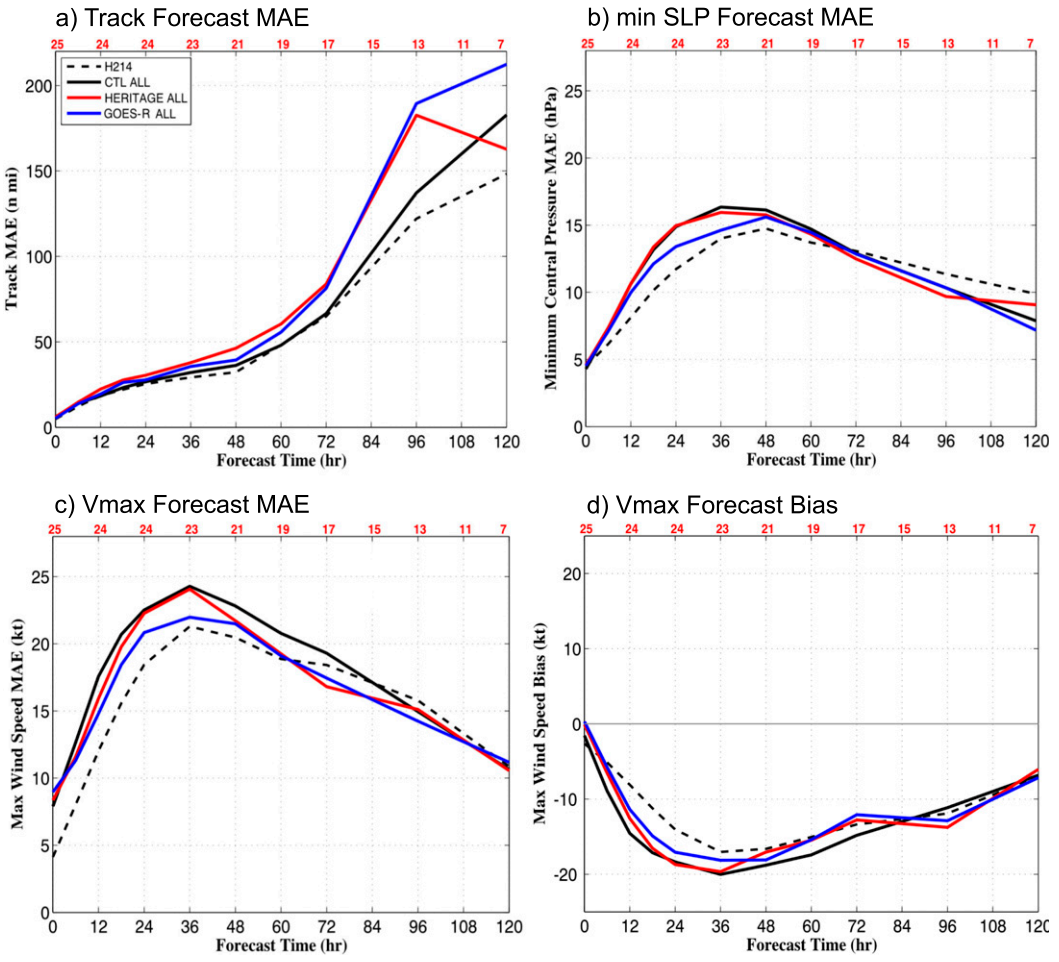

FIG. 9. As in Fig. 5, but for the Hurricane Gonzalo case only.

durable one, at least out to 6 h (cf. Figs. 10f and 10c). It is important to reiterate that the blending process in HWRF DA has a significant impact on the vortex structure used to initiate forecasts. In particular, analysis increments within 150 km of the center are eliminated below 600 hPa in favor of the first-guess structure provided by vortex initialization. Therefore, the increments have little direct impact on the low-level inner-core structure. Rather, any impact is going to be indirect from the outer radii or from the upper levels.

However, to illustrate the degree of caution necessary in interpreting these results, Fig. 11 shows the impact of vortex relocation/correction in arriving at the 0600 UTC background fields. The raw forecasts on d03 for CTL and GOES-R are shown in Figs. 11a and 11c, respectively, and their counterparts after relocation/correction are shown in Figs. 11b and 11d. As is seen, the relocated CTL vortex is more upright than in the raw forecasts, while the GOES-R vortex requires a much less severe correction. While this speaks favorably to the GOES-R impact (i.e., the raw forecast was in better agreement with the TCVitals), the severe correction to the CTL vortex structure highlights the difficulty of impact attribution (and of comparing impacts among various experiments) in a cycled HWRF DA setting.

There is also some interesting behavior in the results if partitioned by cycle time. Figure 12 shows that the model intensity biases are strongly negative for the combined sample, except at $T = 0$ h (and at $T = 120$ h, but the sample sizes become very small). The assimilation of AMVs results in a positive bias at the initial time, but only with the 1200 and 1800 UTC cycles. This influence is apparent through the 24-h forecast lead time in both AMV datasets, thereafter continuing with the GOES-R results as a small mitigation of the CTL negative bias through the rest of the lead times. Interestingly, it is during these times that the VIS AMVs are dominant (Fig. 13). The VIS AMVs are only produced at low levels [capped at 700 hPa; Velden et al. (2005)], and are usually found outside the TC core

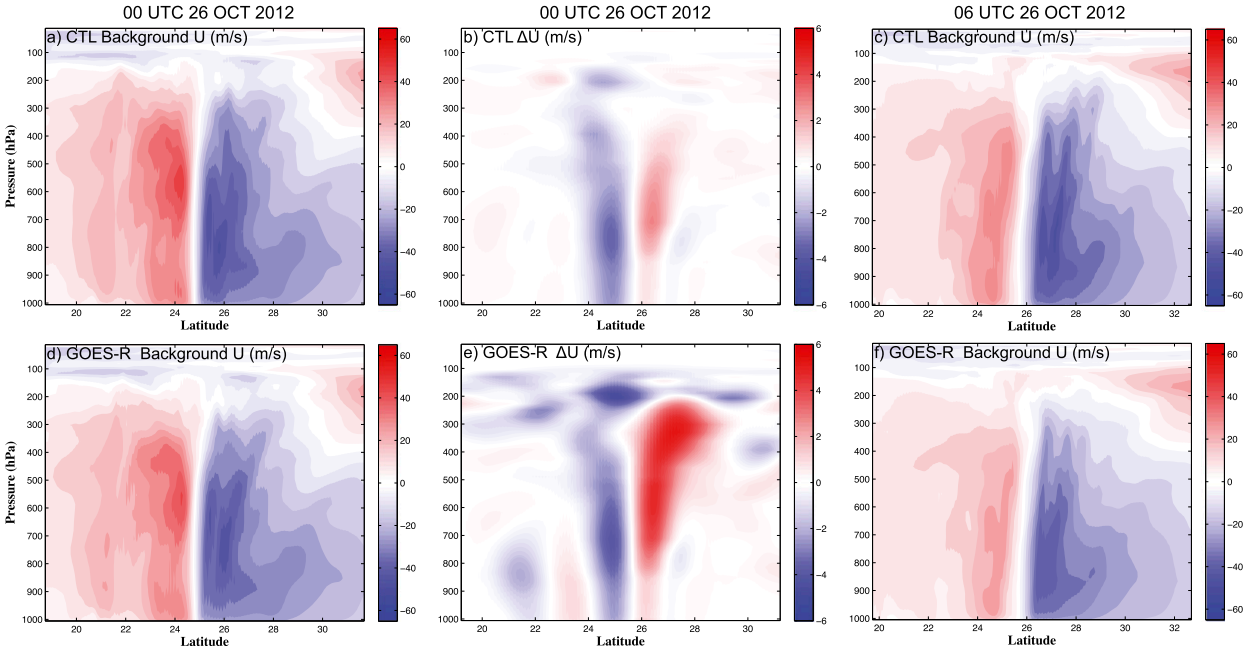

FIG. 10. Vertical cross sections of zonal wind at 0000 UTC 26 Oct 2012 during Hurricane Sandy along 76°W facing west for (left) HWRF background analyses, (middle) analysis increments, and (right) the background analyses in the subsequent cycle (6-h forecast). Plots are shown for both the (a)–(c) CTL and (d)–(f) for the assimilated GOES-R AMV experiments and are computed on expanded domain d02. Warm (cold) colors indicate westerly (easterly) winds. The core of Sandy is located at about 25°N.

region due to convection and cirrus obscuration of low-level cloud targets. This could suggest that the VIS AMV data are influencing the model TC vortex outer wind radii, which then can influence the model intensity after continuous assimilation cycles.

5. Discussion and summary

Satellite-derived atmospheric motion vectors (AMVs) are becoming increasingly available in quantities and quality commensurate with high-resolution TC forecast systems. Fully exploiting the information content of the AMVs in TC data assimilation is a current challenge. Recent studies using research models suggest that enhanced AMVs, when assimilated in a continuous mode, can improve TC initial analyses and track/intensity forecasts. However, the case-by-case forecast impacts have been mixed, and positive results are generally modest.

In this study, we investigate the assimilation of enhanced (higher resolution) AMV datasets for impact in the NCEP operational hurricane forecast model HWRF. Forecasts of Atlantic tropical cyclone track and intensity are examined for impact by inclusion of the enhanced AMVs via direct continuous data assimilation. Experiments are conducted for two AMV derivation methodologies (''HERITAGE'' and ''GOES-R''), and also for varying levels of quality control in order to assess and inform the optimization of the AMV assimilation process in HWRF. Our study is meant as exploratory and will require the benefit of a much larger sample to confirm the findings. Results are presented for three selected Atlantic tropical cyclone events and compared to Control forecasts without the enhanced AMVs as well as the corresponding operational HWRF forecasts.

Our findings indicate that the direct assimilation of high-resolution AMVs have an overall modest positive impact on HWRF forecasts, but the impact magnitudes are dependent on the 1) availability of rapid-scan imagery used to produce the AMVs, 2) AMV derivation approach, 3) level of quality control employed in the assimilation, and 4) vortex initialization procedure and likely the degree to which unbalanced states are allowed to enter the model analyses via the AMV observations.

The promising aspects of the findings are related to the first three. There is some suggestion that the AMVs derived from rapid-scan imaging may impart greater positive model forecast impact [supported by previous studies; Wu et al. (2014, 2015)]. These rapid scans will become a routine image sampling strategy once *GOES-16* is commissioned in 2017. It is also apparent that the new AMV derivation approach developed as part of GOES-R readiness is capable of reproducing results comparable to the current operational (HERITAGE) method. In fact, when coupled with the GSI QC as part

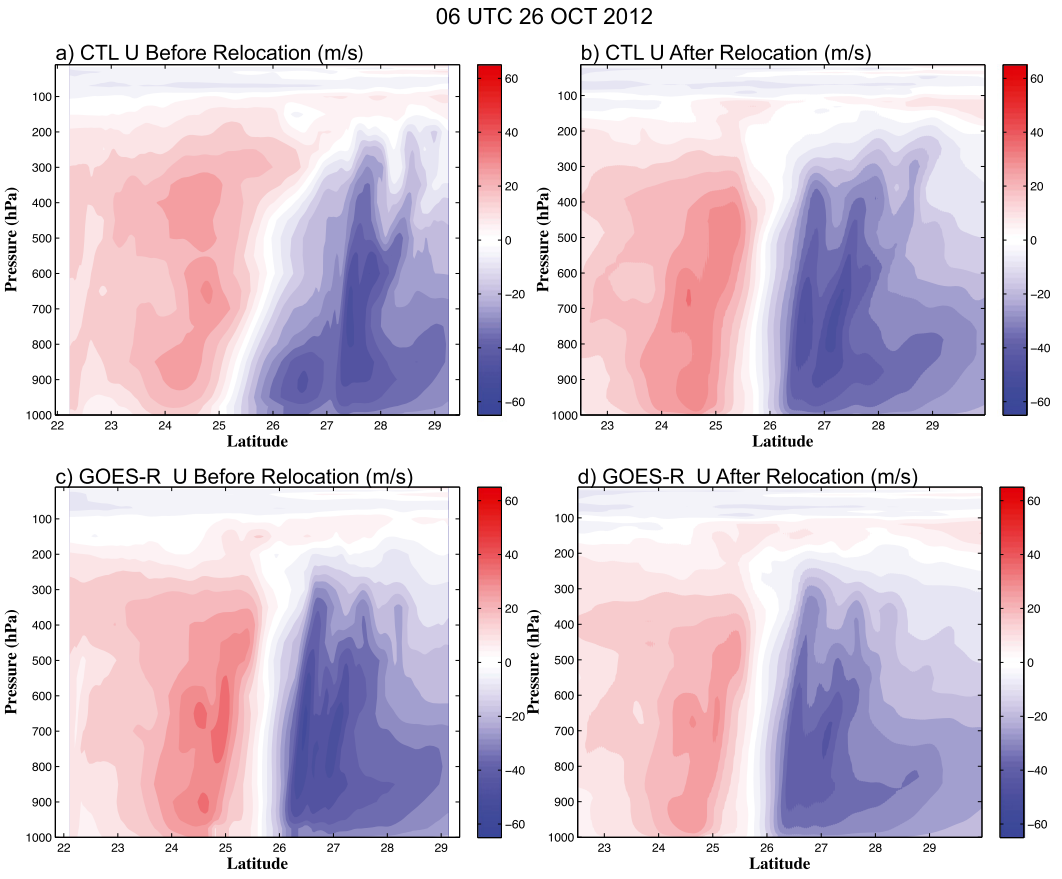

FIG. 11. Vertical cross sections of zonal wind for CTL and GOES-R (as in Fig. 10), but for background fields (a),(c) before and (b),(d) after vortex relocation is applied on the innermost forecast domain (i.e., d03). (a),(c) The 6-h forecasts and (b),(d) the impacts of vortex relocation as well as size and intensity adjustment.

of the HDAS, the forecast results are superior to HERITAGE in most cases examined. This is a pleasing result given the GOES-R AMV processing algorithm is on an operational path at NOAA/NESDIS.

The overall HWRF forecast impact results from our study are neutral to only slightly positive, which for TC track is acceptable since the HWRF CTL/operational forecasts were already quite good. The HWRF does not

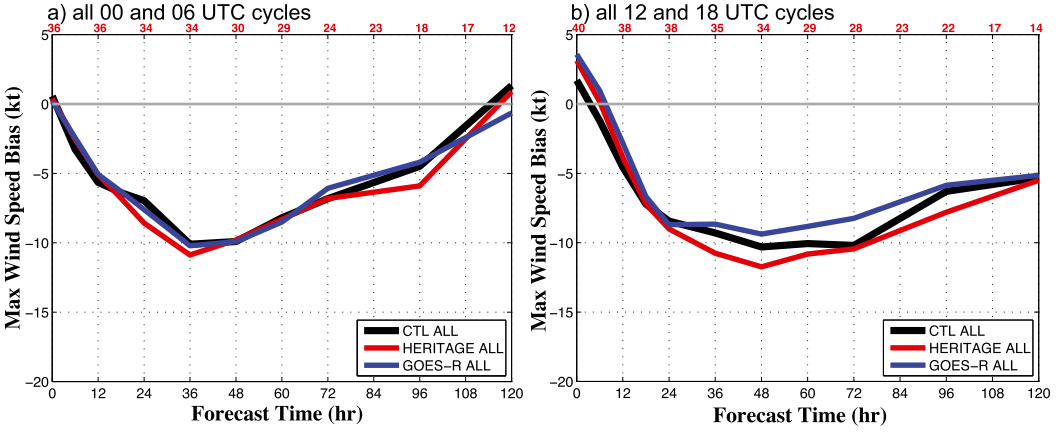

FIG. 12. HWRF intensity (maximum sustained wind speed) bias forecast errors (mean absolute errors) for the combined results of the three TC cases, partitioned by analysis cycle time. (a) 0000 and 0600 UTC cycles and (b) 1200 and 1800 UTC cycles. Sample sizes for each forecast lead time are indicated in red along the top of the plot.

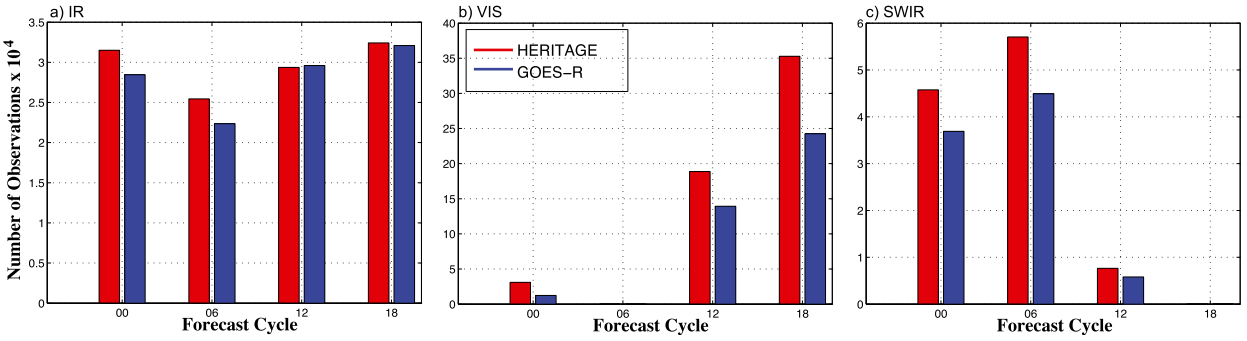

FIG. 13. Number of AMV observations assimilated by analysis cycle, partitioned by AMV type. "IR" includes both IR-window and CTWV vectors. VIS (daylight hours) and SWIR (nondaylight hours) AMVs are only produced in the lower troposphere (700–950 hPa).

perform hybrid GSI DA on its parent domain (d01), which covers the synoptic/large-scale features such as the environmental steering flow that governs much of the track of hurricanes. Recall that the AMVs are currently only assimilated in the HDAS inner domains (d02/d03, Fig. 1). Without assimilating AMVs in the large domain, it is likely that HWRF track forecast improvement will be more difficult since there is little new information being added to the analysis of the broader-scale environmental steering flow. There is some degradation in the longer-range lead times (≥96 h), although this result is derived from a fairly small sample size. We speculate that the longer forecast times may be feeling the influence of d02/d01 analysis boundaries. Given the high density of the data, especially when there are rapid-scan-produced AMVs available, it is possible domain interface issues could arise in the initial analyses that propagate into the longer-range forecasts of the TC. For example, TCs Sandy and Gonzalo both produced some HWRF track forecast degradations at 96 h and beyond, and had very high density AMVs from rapid scans. Future studies could explore the assimilation of AMVs in the parent domain since the observations are operationally available over those scales.

The AMVs had more opportunity to correct the TC intensity biases in the HWRF forecasts (particularly the short term) from the three selected cases, and modest impacts are noted. There are many potential reasons for a lack of stronger impact. Unlike TC track, which is controlled primary by the environmental steering flow, TC intensity modulation is governed more by near-storm or in-storm processes. The current configuration of the HWRF invokes vortex relocation, size and intensity correction, and merging/blending procedures at each 6-h cycle. As part of this suite of pre- and post-DA processing techniques, the information content of previous-time analysis cycles is lost before DA occurs and the information content of current-time, data-influenced analyses increments are removed in the core region due to imbalances (model bias/covariance). Obviously, this is a suboptimal use of AMV observations near the core region, and this is certainly an area of current/future investigation for the HWRF DA team. Cycled covariances will better represent mesoscale flows to take advantage of the enhanced AMV datasets, along with more frequent DA cycling (i.e., 1 h vs 6 h). Replacing the vortex initialization with self-consistent DA involving hybrid/EnKF steps and novel inner-core observations (satellite, aircraft) is being explored.

There are certainly other plausible reasons for the modest AMV impact on the model vortex winds, including mass balance constraints and the model expectation of vertically supported profiles (of which the AMVs are not). It is also possible given the density of the AMV datasets and their assimilation at hourly increments, that the data are being overfitted in the analysis. Correlated error is always a concern. This study disregarded preassimilation GSI thinning procedures with the goal of better-resolving true hurricane-scale flow fields, but this is a topic for future investigation as well. The same goes for tuning of the covariance length scales in GSI, as different observation types such as AMVs (which possess marked differences in spatio-temporal density) may benefit from some adjustment to the default settings. Despite the sometimes mixed impacts, there are good lessons to be learned from this investigation, and as such the prospects of direct assimilation of enhanced AMVs into HWRF in the GOES-R series era are promising.

Acknowledgments. The authors thank Vijay Tallapragada of NCEP/EMC for support and guidance on the HWRF experiments, and two reviewers including Jason Sippel of NCEP/EMC for very helpful comments. All of the simulations, data assimilation, and subsequent analysis of all results were performed on NOAA's Jet supercomputing system with support from the Hurricane Forecast Improvement Project (HFIP).

This research was supported by NOAA/NESDIS/HFIP Grant NA10NES4400013 and GOES-R Program Office Contract DG133E-12-CQ-0021.

REFERENCES

Berger, H., R. Langland, C. S. Velden, C. Reynolds, and P. M. Pauley, 2011: Impact of enhanced satellite-derived atmospheric motion vector observations on numerical tropical cyclone track forecasts in the western North Pacific during TPARC/TCS-08. *J. Appl. Meteor. Climatol.*, **50**, 2309–2318, doi:10.1175/JAMC-D-11-019.1.

Blake, E., T. Kimberlain, R. Berg, J. Cangiolosi, and J. Beven II, 2013: Tropical Cyclone Report: Hurricane Sandy (AL182012). National Hurricane Center Tropical Cyclone Rep. AL182012, 157 pp. [Available online at http://www.nhc.noaa.gov/data/tcr/AL182012_Sandy.pdf.]

Borde, R., M. Doutriaux-Boucher, G. Dew, and M. Carranza, 2014: A direct link between feature tracking and height assignment of operational EUMETSAT atmospheric motion vectors. *J. Atmos. Oceanic Technol.*, **31**, 33–46, doi:10.1175/JTECH-D-13-00126.1.

Bresky, W., J. Daniels, A. Bailey, and S. Wanzong, 2012: New methods toward minimizing the slow speed bias associated with atmospheric motion vectors. *J. Appl. Meteor. Climatol.*, **51**, 2137–2151, doi:10.1175/JAMC-D-11-0234.1.

Brown, D., 2015: Hurricane Gonzalo (AL082014). National Hurricane Center Tropical Cyclone Rep. AL082014, 30 pp. [Available online at http://www.nhc.noaa.gov/data/tcr/AL082014_Gonzalo.pdf.]

Fels, S. B., and M. D. Schwarzkopf, 1975: The simplified exchange approximation: A new method for radiative transfer calculations. *J. Atmos. Sci.*, **32**, 1475–1488, doi:10.1175/1520-0469(1975)032<1475:TSEAAN>2.0.CO;2.

Ferrier, B. S., 2005: An efficient mixed-phase cloud and precipitation scheme for use in operational NWP models. *Eos, Trans. Amer. Geophys. Union*, **86** (Spring Meeting Suppl.), Abstract A42A-02.

Goerss, J. S., 2009: Impact of satellite observations on the tropical cyclone track forecasts of the Navy Operational Global Atmospheric Prediction System. *Mon. Wea. Rev.*, **137**, 41–50, doi:10.1175/2008MWR2601.1.

Han, J., and H.-L. Pan, 2011: Revision of convection and vertical diffusion schemes in the NCEP Global Forecast System. *Wea. Forecasting*, **26**, 520–533, doi:10.1175/WAF-D-10-05038.1.

Holmlund, K., C. S. Velden, and M. Rohn, 2001: Enhanced automated quality control applied to high-density satellite-derived winds. *Mon. Wea. Rev.*, **129**, 517–529, doi:10.1175/1520-0493(2001)129<0517:EAQCAT>2.0.CO;2.

Hong, S.-Y., and H.-L. Pan, 1996: Nonlocal boundary layer vertical diffusion in a medium-range forecast model. *Mon. Wea. Rev.*, **124**, 2322–2339, doi:10.1175/1520-0493(1996)124<2322:NBLVDI>2.0.CO;2.

Lacis, A. A., and J. E. Hansen, 1974: A parameterization for the absorption of solar radiation in the earth's atmosphere. *J. Atmos. Sci.*, **31**, 118–133, doi:10.1175/1520-0469(1974)031<0118:APFTAO>2.0.CO;2.

Langland, R. H., C. Velden, P. M. Pauley, and H. Berger, 2009: Impact of satellite-derived rapid-scan wind observations on numerical model forecasts of Hurricane Katrina. *Mon. Wea. Rev.*, **137**, 1615–1622, doi:10.1175/2008MWR2627.1.

Le Marshall, J., J. Jung, T. Zapotocny, C. Redder, M. Dunn, J. Daniels, and L. P. Riishojgaard, 2008a: Impact of MODIS atmospheric motion vectors on a global NWP system. *Aust. Meteor. Mag.*, **57**, 45–51.

——, R. Seecamp, M. Dunn, C. Velden, S. Wanzong, K. Puri, R. Bowen, and A. Rea, 2008b: The contribution of locally generated MTSat-1R atmospheric motion vectors to operational meteorology in the Australian region. *Aust. Meteor. Mag.*, **57**, 359–365.

McNally, T., M. Bonavita, and J.-N. Thepaut, 2014: The role of satellite data in the forecasting of Hurricane Sandy. *Mon. Wea. Rev.*, **142**, 634–646, doi:10.1175/MWR-D-13-00170.1.

Nebuda, S., J. Jung, D. Santek, J. Daniels, and W. Bresky, 2014: Assimilation of GOES-R atmospheric motion vectors in the NCEP Global Forecast System. *Proc. 12th Int. Winds Workshop*, Copenhagen, Denmark, IWWG, IWW12. [Available online at http://cimss.ssec.wisc.edu/iwwg/iwwg_meetings.html.]

Pu, Z., X. Li, C. S. Velden, S. D. Aberson, and W. T. Liu, 2008: The impact of aircraft dropsonde and satellite wind data on numerical simulations of two landfalling tropical storms during the tropical cloud systems and processes experiment. *Wea. Forecasting*, **23**, 62–79, doi:10.1175/2007WAF2007006.1.

Schwarzkopf, M. D., and S. Fels, 1991: The simplified exchange method revisited: An accurate, rapid method for computation of infrared cooling rates and fluxes. *J. Geophys. Res.*, **96**, 9075–9096, doi:10.1029/89JD01598.

Sears, J., and C. Velden, 2012: Validation of satellite-derived atmospheric motion vectors and analyses around tropical disturbances. *J. Appl. Meteor. Climatol.*, **51**, 1823–1834, doi:10.1175/JAMC-D-12-024.1.

Stewart, S., 2014: Hurricane Edouard (AL062014). National Hurricane Center Tropical Cyclone Rep. AL062014, 19 pp. [Available online at http://www.nhc.noaa.gov/data/tcr/AL062014_Edouard.pdf.]

Tallapragada, V., and Coauthors, 2014: Hurricane Weather Research and Forecasting (HWRF) Model: 2014 scientific documentation. NCAR Development Testbed Center Rep. HWRF v3.6a, 105 pp. [Available online at http://www.dtcenter.org/HurrWRF/users/docs/scientific_documents/HWRFv3.6a_ScientificDoc.pdf.]

Tuleya, R. E., 1994: Tropical storm development and decay: Sensitivity to surface boundary conditions. *Mon. Wea. Rev.*, **122**, 291–304, doi:10.1175/1520-0493(1994)122<0291:TSDADS>2.0.CO;2.

Velden, C. S., C. M. Hayden, S. J. Nieman, W. P. Menzel, S. Wanzong, and J. S. Goerss, 1997: Upper-tropospheric winds derived from geostationary satellite water vapor observations. *Bull. Amer. Meteor. Soc.*, **78**, 173–195, doi:10.1175/1520-0477(1997)078<0173:UTWDFG>2.0.CO;2.

——, T. L. Olander, and S. Wanzong, 1998: The impact of multispectral *GOES-8* wind information on Atlantic tropical cyclone track forecasts in 1995. Part I: Dataset methodology, description, and case analysis. *Mon. Wea. Rev.*, **126**, 1202–1218, doi:10.1175/1520-0493(1998)126<1202:TIOMGW>2.0.CO;2.

——, and Coauthors, 2005: Recent innovations in deriving tropospheric winds from meteorological satellites. *Bull. Amer. Meteor. Soc.*, **86**, 205–223, doi:10.1175/BAMS-86-2-205.

Wang, X., 2010: Incorporating ensemble covariance in the Gridpoint Statistical Interpolation (GSI) variational minimization: A mathematical framework. *Mon. Wea. Rev.*, **138**, 2990–2995, doi:10.1175/2010MWR3245.1.

Wu, T. C., H. Liu, S. Majumdar, C. Velden, and J. Anderson, 2014: Influence of assimilating satellite-derived atmospheric motion

vector observations on numerical analyses and forecasts of tropical cyclone track and intensity. *Mon. Wea. Rev.*, **142**, 49–71, doi:10.1175/MWR-D-13-00023.1.

——, C. Velden, S. Majumdar, H. Liu, and J. Anderson, 2015: Understanding the influence of assimilating subsets of enhanced atmospheric motion vectors on numerical analyses and forecasts of tropical cyclone track and intensity with an ensemble Kalman Filter. *Mon. Wea. Rev.*, **143**, 2506–2531, doi:10.1175/MWR-D-14-00220.1.

Wu, W.-S., R. J. Purser, and D. F. Parrish, 2002: Three-dimensional variational analysis with spatially inhomogeneous covariances. *Mon. Wea. Rev.*, **130**, 2905–2916, doi:10.1175/1520-0493(2002)130<2905:TDVAWS>2.0.CO;2.

Yablonsky, R. M., I. Ginis, and B. Thomas, 2015: Ocean modeling with flexible initialization for improved coupled tropical cyclone-ocean prediction. *Environ. Modell. Software*, **67**, 26–30, doi:10.1016/j.envsoft.2015.01.003.

Yamashita, K., 2012: An observing system experiment of MTSAT rapid scan AMV using JMA meso-scale operational NWP system. *Proc. 11th Int. Winds Workshop*, Auckland, New Zealand, IWWG, IWW11. [Available online at http://cimss.ssec.wisc.edu/iwwg/iwwg_meetings.html.]